tvst

Article

Optogenetic Modulation of Intraocular Pressure in a Glucocorticoid-Induced Ocular Hypertension Mouse Model

Tia J. Kowal[1,*], Philipp P. Prosseda[1,*], Ke Ning[1], Biao Wang[1], Jorge Alvarado[1], Brent E. Sendayen[1], Sayena Jabbehdari[1,2], W. Daniel Stamer[4], Yang Hu[1], and Yang Sun[1,3]

[1] Department of Ophthalmology, Stanford University School of Medicine, Palo Alto, CA, USA
[2] Department of Ophthalmology and Visual Sciences, University of Illinois at Chicago, Chicago, Illinois, USA
[3] Palo Alto Veterans Administration, Palo Alto, CA, USA
[4] Duke Eye Center, Department of Ophthalmology, Duke University, Durham, NC, USA

Correspondence: Yang Sun, Department of Ophthalmology, Stanford University School of Medicine, 1651 Page Mill Road, Rm 2220, Palo Alto, CA 94306, USA.
e-mail: yangsun@stanford.edu

Received: November 9, 2020
Accepted: March 22, 2021
Published: May 6, 2021

Keywords: steroid-induced glaucoma; dexamethasone, intraocular pressure; inositol phosphatase; primary cilia

Citation: Kowal TJ, Prosseda PP, Ning K, Wang B, Alvarado J, Sendayen BE, Jabbehdari S, Stamer WD, Hu Y, Sun Y. Optogenetic modulation of intraocular pressure in a glucocorticoid-induced ocular hypertension mouse model. Transl Vis Sci Technol. 2021;10(6):10, https://doi.org/10.1167/tvst.10.6.10

Purpose: Steroid-induced glaucoma is a common form of secondary open angle glaucoma characterized by ocular hypertension (elevated intraocular pressure [IOP]) in response to prolonged glucocorticoid exposure. Elevated IOP occurs with increased outflow resistance and altered trabecular meshwork (TM) function. Recently, we used an optogenetic approach in TM to regulate the 5-phosphatase, OCRL, which contributes to regulating PI(4,5)P2 levels. Here, we applied this system with the aim of reversing compromised outflow function in a steroid-induced ocular hypertension mouse model.

Methods: Elevated IOP was induced by chronic subconjunctival dexamethasone injections in wild-type C57Bl/6j mice. AAV2 viruses containing optogenetic modules of cryptochrome 2 (Cry2)-OCRL-5ptase and CIBN-GFP were injected into the anterior chamber. Four weeks after viral expression and dexamethasone exposure, IOP was measured by tonometer and outflow facility was measured by perfusion apparatus. Human TM cells were treated with dexamethasone, stimulated by light and treated with rhodamine-phalloidin to analyze actin structure.

Results: Dexamethasone treatment elevated IOP and decreased outflow facility in wild-type mice. Optogenetic constructs were expressed in the TM of mouse eyes. Light stimulation caused CRY2-OCRL-5ptase to translocate to plasma membrane (CIBN-CAAX-GFP) and cilia (CIBN-SSTR3-GFP) in TM cells, which rescued the IOP and outflow facility. In addition, aberrant actin structures formed by dexamethasone treatment were reduced by optogenetic stimulation in human TM cells in culture.

Conclusions: Subcellular targeting of inositol phosphatases to remove PIP2 represents a promising strategy to reverse defective TM function in steroid-induced ocular hypertension.

Translational Relevance: Targeted modulation of OCRL may be used to decrease steroid-induced elevated IOP.

Introduction

Corticosteroids are widely used in the eye clinic owing to their anti-inflammatory and anti-angiogenic properties.[1–6] However, the therapeutic use of glucocorticoids can cause elevated intraocular pressure (IOP) and vision loss, called steroid-induced glaucoma.[1] An elevated IOP after dose-dependent corticosteroid treatment can occur regardless of the delivery route; the pathophysiology of this condition remains unclear.[7–21]

Physiologic IOP is maintained by regulating the production of aqueous humor by the ciliary body and drainage of the aqueous humor by the trabecular meshwork (TM). Similar to phenotypes observed in primary open-angle glaucoma, the exposure of conventional outflow cells to steroids has been reported to induce changes to the TM that may ultimately impair TM function. Several corticosteroid-induced

ocular hypertension and glaucoma animal models have already been developed.[22–29] The anatomic and physiologic features of murine Schlemm's canal, outflow pathway, and TM are similar to those of humans,[30] and corticosteroid induced ocular hypertension has been reported to be analogous in mice and humans.[30–34] Here we used an established method of dexamethasone-induced ocular hypertension that mimics the effects observed in human steroid-induced glaucoma, including decreased outflow facility, elevated IOP, and altered actin cytoskeleton morphology in TM cells.[24,26,30,34–36]

Primary cilia have recently been shown to play a role in TM regulation of outflow facility.[37] They are immotile cellular projections that are thought to function as sensory antenna-like organelles that detect and transduce extracellular stimuli into intracellular signals which regulate cell growth, differentiation, and tissue homeostasis.[38] Interestingly, congenital glaucoma occurs in patients with Lowe syndrome, a rare X-linked ciliopathy that presents with congenital cataracts, renal failure, and developmental delay.[39] Lowe syndrome is caused by mutations in the gene encoding for the inositol 5-phosphatase, OCRL,[40–42] which contributes to regulating cellular levels of PI(4,5)P2 by hydrolyzing PI(4,5)P2 and PI(3,4,5)P3.[41,43] The presence of PI(4,5)P2 at the membrane can promote actin polymerization, whereas its loss results in actin depolymerization. Because some steroids, including dexamethasone, have been shown to cause the formation of crossed-linked actin networks (CLANS), we propose that targeting OCRL to subcellular compartments will decrease the levels of PI(4,5)P2, causing actin depolymerization and rescuing the cytoskeletal defects produced by dexamethasone exposure.

Here, we express the cryptochrome 2 (CRY2)/CIBN optogenetic system in the TM of steroid-induced ocular hypertension mice eyes and show that regulating localization of the OCRL 5-phosphatase domain (5-ptase) to specific subcellular compartments reduces IOP and increases outflow facility. In addition, aberrant actin structures formed by dexamethasone treatment were decreased by optogenetic stimulation in human TM (HTM) cells in culture.

Methods

Reagents

Alexa568-Phalloidin and ProLong Gold Antifade Mountant with DAPI were purchased from Invitrogen (Carlsbad, CA). Dexamethasone (D2915) was purchased from Tocris.

Animals

All in vivo experiments followed the guidelines of the Association for Research in Vision and Ophthalmology Statement for the Use of Animals in Ophthalmic and Vision Research and were approved by the Institutional Animal Care and Use Committee of Stanford University School of Medicine. All wild-type (C57BL/6j) mice were purchased from The Jackson Laboratories (Bar Harbor, ME). To avoid age-related variability, all mice were within the same age range. Mice were kept under a 12-hour light/dark cycle and had free access to water and food. Ketamine injections were based on mouse body weight (100 mg/kg). Mice were anesthetized by isoflurane for the blue light exposure and tonometer readings. Oxygen flow was set to 2 L/min; isoflurane was 1% and delivered by nose cone.

Cell Culture

HTM cells were obtained from cadaveric corneas (Indiana Lions Eye Bank, Nora, IN); characterization and culturing protocols were based upon established methodology in the field.[44,45]

DNA Plasmid and Transfection

CIBN-EGFP-CAAX and mCherry-CRY2-OCRL were generously provided by Pietro de Camilli (Yale University). Somatostatin receptor 3 (SSTR3) ciliary targeting sequence was cloned into CIBN-EGFP as previously described.[46] Lipofectamine 3000 (Invitrogen) or polyethylenimine (Sigma, St Louis, MO) was used to transfect optogenetic constructs or subclone them separately into AAV2.

Immunofluorescence

Cells grown on eight-well chamber slides were activated using a 488-nm blue laser as described previously[46] and fixed in 4% PFA for 10 minutes at room temperature. Cells were permeabilized with 0.2% Triton X-100 and incubated with rhodamine-phalloidin (Invitrogen R415) diluted 1:200 in blocking solution (0.5% bovine serum albumin, 10% normal goat serum in phosphate-buffered saline) for 1 hour at room temperature.

Quantification of CLANs Positive Cells

Cells were imaged and counted according to the method described by Filla et al.[47] In brief, cells stained with rhodamine-phalloidin were imaged using a 20× objective. Cells with three bright spokes of actin filaments that connected at a point were considered to have CLANs. The total number of cells in an image expressing CIBN-CAAX-GFP and the total number of CLANs-positive cells expressing CIBN-CAAX-GFP were counted in an *n* of 3 replicate studies with approximately 40 cells per group (blue light, no light) counted for each replicate.

Confocal Microscopy and Live Cell Imaging

Imaging was performed with a Zeiss LSM880 confocal microscope (Carl Zeiss Meditec, Jena, Germany). Using 2% of total laser output, blue laser was administered by taking a Z-stack picture with the single 488-nm (for CIBN-GFP) channel, followed by time series Z-stack scanning of the mCherry channel for at least 10 minutes. ImageJ was used to quantify the intensity of mCherry-CRY2-OCRL in various experiments by measuring both the area and total fluorescence intensity in the selected area of interest (v1.47v, NIH, Bethesda, MD).

Dexamethasone-Induced Ocular Hypertension

Dexamethasone-induced ocular hypertension was generated according to published protocols.[24,26,34–36,48] A 10 mg/mL solution of dexamethasone (Sigma D2915) was prepared using sterilized d-water. For the subconjunctival injections, the lower eyelid was retracted and the conjunctiva gently pulled away from the surface of the globe using forceps. Then, 20 µL of the dexamethasone suspension was injected immediately under the conjunctiva over 20 to 25 seconds using a 32G needle. The subconjunctival injections were performed weekly in both eyes of each animal.

Intraocular Injection

Intraocular injections were performed as previously described by Wang et al.[49] Briefly, AAVs with optogenetic constructs were injected into the anterior chamber of the eye under ketamine anesthesia. As a local anesthetic, 1 drop of 0.5% proparacaine hydrochloride (Bausch & Lomb, Tampa, FL) was applied to each eye. To create a small aperture to the anterior chamber, the cornea was punctured using a sterile 33G needle (STERiJECT) under a dissection microscope (Nikon, Tokyo, Japan). After removing the needle, a fine borosilicate glass capillary (World Precision Instruments 1B150-4; Sarasota, FL) was connected to a Hamilton syringe using polyethylene tubing and passed through the same hole to introduce a small air bubble. The capillary was slowly removed and filled with 2-µL viral constructs (10^{10} infectious U/µL) diluted in Fast Green blue dye to monitor the injection through the puncture site. The capillary was then reinserted, and the anterior chamber filled with the distinct blue tint of the virus. The glass capillary was kept in position to monitor the pattern of the staining. To prevent leakage of the virus and to seal off the puncture site, the air bubble was gently moved to the insertion site. At the end of the procedure, neomycin was applied to decrease the risk of infection.

Measurement of IOP

The Icare TonoLab tonometer (TV02; Icare Finland Oy, Espoo, Finland) was used to measure the IOP. Briefly, mice were anesthetized by nose cone delivery of isoflurane and oxygen. Each eye received 1 drop of proparacaine topical anesthesia, and the IOP was measured 1 minute later. The mean of five readings was recorded as the IOP.

Mouse Eye Perfusion Apparatus

For the eye perfusion, mice were anesthetized and treated when necessary (optogenetic activation) and subsequently sacrificed by cervical dislocation. Within 10 minutes of death, mouse eyeballs were enucleated and perfused immediately.

The eye perfusion apparatus was designed as previously described.[50,51] As shown in Figure 1B, a 5-mm-long 33G needle (TSK Laboratory, Tochigi, Japan) attached to a micromanipulator was introduced into the anterior chamber. The needle was connected to a rigid and noncompliant tube (Lectro-cath) attached to a three-way stopcock. The three-way stopcock was connected to a calibrated glass Hamilton syringe driven by a New Era syringe pump (Syringe Pump, Farmingdale, NY) on one hub and an MLT1199-BP transducer (AD Instruments, Colorado Springs, CO), which was connected to an amplifier by a Transducer Cable Kit (AD Instruments), on the other. The Amplifier/PowerLab system (AD Instruments) was connected to a computer running the LabChart8 software (AD Instruments), which integrated with custom pumping software to control the pump flow within a range from 0.001 to 2120.000 mL/h. Before each experiment, the

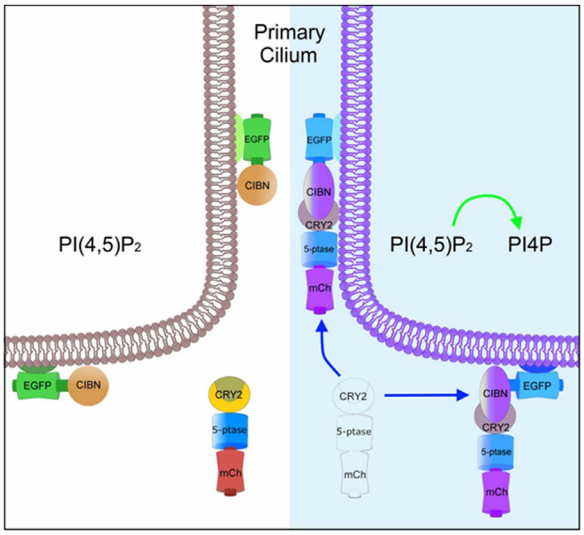

Figure 1. Overview of Cry2-CIBN optogenetic system. Schematic representation of the optogenetic recruitment model of mCh-CRY2-5-ptase to primary cilium or plasma membrane after blue light illumination. Optogenetic activation recruits cytosolic mCh-CRY2-5-ptase to its dimerization partner EGFP-CIBN, which is targeted to specific subcellular compartments.

perfusion apparatus was filled with sterile Dulbecco's phosphate-buffered saline and calibrated.

The pressure before cannulation was zero referenced; the pressure after cannulation was transduced into the anterior chamber by the pressure transducer. The low-speed flow rate was controlled by the syringe pump and automatically adjusted according to the feedback between the LabChart8 software and the pumping software. When the pressure reached a stable value, outflow from the anterior chamber was recorded. To maintain a constant and stable IOP over 10 minutes for each pressure value, the eye displayed a constant pressure of 10 to 35 mm Hg (Y-value) and related flow rate (X-value). X1 and Y1 indicate a paired perfusion pressure and its corresponding IOP (10, 15, 20, 25, and 30 mm Hg). The IOP was then plotted against its corresponding stable flow rate, where the slope indicates conventional outflow facility and the Y-intercept the uveoscleral outflow independent of IOP. Average outflow facility of perfused eyes with flow rate (μL/min) on the Y-axis plotted against IOP (in mm Hg) on the X-axis represents the perfusion plot of IOP versus flow rate.

Eyes were perfused over 50 minutes at increments of IOP. To determine the outflow facility of each sample and the association between IOP and corresponding outflow rate, the modified Goldmann equation ($F = C^*IOP + U$) was used. In this equation, C is the conventional outflow rate. GraphPad Prism was used to plot the recorded flow rates and the corresponding IOPs, and the conventional outflow rate (C) of each sample was calculated.

AAV2-S-Vector Construction and Production

AAV2-s vector was designed to target the HTM cells as described by Prosseda et al.,[46,52] and viral purification were routinely prepared by the triple plasmid transfection method as previously described by Wang et al.[49] and Lock et al.,[53] respectively. Briefly, capsid (p-Acg2), transgene, and helper (p-helper) plasmids (ratio 1:1:1) were transfected using PolyJet In Vitro DNA Transfection Reagent in HEK293 cells. Viral particles were collected by precipitation in 40% polyethylene glycol and purified by cesium chloride density gradient. Viral particles were dialyzed, and AAV2-s titer determined by SYBR green quantitative PCR amplification using primers and probes detecting the promoter and transgene of the transgene cassette with DNase-I-resistant vector genome copies as a reference.

Statistical Analysis

Statistical analyses were performed using Graphpad8 (Prism) software. Results are expressed as mean values ± standard error of the mean. Statistical analyses were performed using linear regression analysis for outflow facility measurement, and unpaired *t*-tests were used to compare the means of two independent groups such as in vivo (outflow facility and IOP between control vs. DEX-treated mice). Paired *t*-tests were used for comparison of blue light illuminated versus nonilluminated eyes of each mouse transduced with optogenetic viruses as indicated. A *P* value of less than 0.05 was considered statistically significant and is indicated by an asterisk.

Results

Optogenetic Targeting of OCRL 5-Phosphatase to Subcellular Compartments

To determine whether subcompartmental distribution of OCRL may influence outflow facility in a steroid-induced ocular hypertension mouse model, we adapted an optogenetic system developed by Idevall-Hagren and Decamilli.[54] The optogenetic system consists of the 5-ptase domain of OCRL fused to one of the optogenetic dimerization partners, CRY2 (hereafter referred to as CRY2-5-ptase$_{OCRL}$). CRY2 can subsequently be directed by light stimulation in a time- and location-specific manner to its dimerizing partner CIBN, which can be targeted to

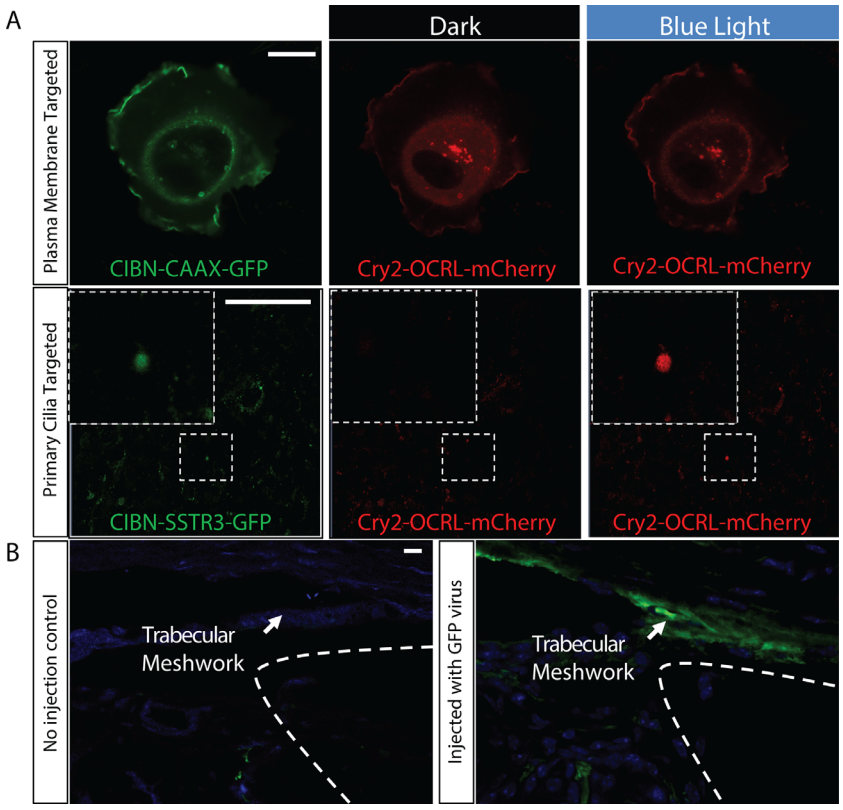

Figure 2. Optogenetic recruitment of OCRL to the plasma membrane and primary cilia and viral infection of the TM. (A) Stimulation with blue light recruits Cry2-OCRL-mCherry to CIBN-CAAX-GFP localized at the plasma membrane (top). Similarly, blue light stimulation causes Cry2-OCRL-mCherry to move to CIBN-SSTR3-GFP targeted at primary cilia (bottom). (B) AAV2-s viral constructs containing the relevant optogenetic constructs: AAV2-s-CRY2-5-ptase$_{OCRL}$ and AAV2-s-CIBN-EGFP-CAAX or AVV2-s-CIBN-EGFP-SSTR3 were injected into the anterior chamber of mice and incubated for 4 weeks. Viral infection was observed in the TM. Scale bar = 20 µm.

different subcellular compartments (Fig. 1A).[46] Importantly, the specificity and reversibility of this system allows for the systematic activation of an enzyme, such as the OCRL 5-ptase, owing to its accumulation in the region of interest. In addition to targeting the plasma membrane (Fig. 2A, top), we modified the optogenetic targeting CIBN construct to specifically target the CRY2-5-ptase$_{OCRL}$ to the primary cilia (Fig. 2A, bottom) to study its functional role in modulating ciliary phosphoinositide levels.[46] For this purpose, we replaced the CIBN-EGFP-CAAX CAAX-box with the ciliary targeting sequence found within the third intracellular loop of the G protein-coupled receptor somatostatin receptor 3 (indicated as SSTR3).[55,56] Using viruses to express these constructs in the TM of mice eyes (Fig. 2B) allowed us to analyze the effect of plasma membrane and ciliary phosphoinositide levels in modulating IOP.

Dexamethasone-Induced Ocular Hypertension Model

To elevate the IOP, we used dexamethasone to induce ocular hypertension in mice, as other investigators have done previously.[24,26,30,35,36] Dexamethasone was administered once weekly over 4 weeks by subconjunctival injections into both eyes (Fig. 3A). We monitored the IOP using rebound tonometry. Tonometer readings at 4 weeks showed a marked increase in the IOP in dexamethasone-treated eyes (18–22 mm Hg), compared with normal baseline untreated IOP (13–16 mm Hg) (Fig. 3B), supporting the validity of the dexamethasone IOP model. At 4 weeks, perfusion analysis of eyes of the dexamethasone treated group demonstrated a significant decrease in outflow facility (1 nL/min/mm Hg) compared with wild-type untreated eyes (5 nL/min/mm Hg), confirming the efficacy of the model (Figs. 3C, D).

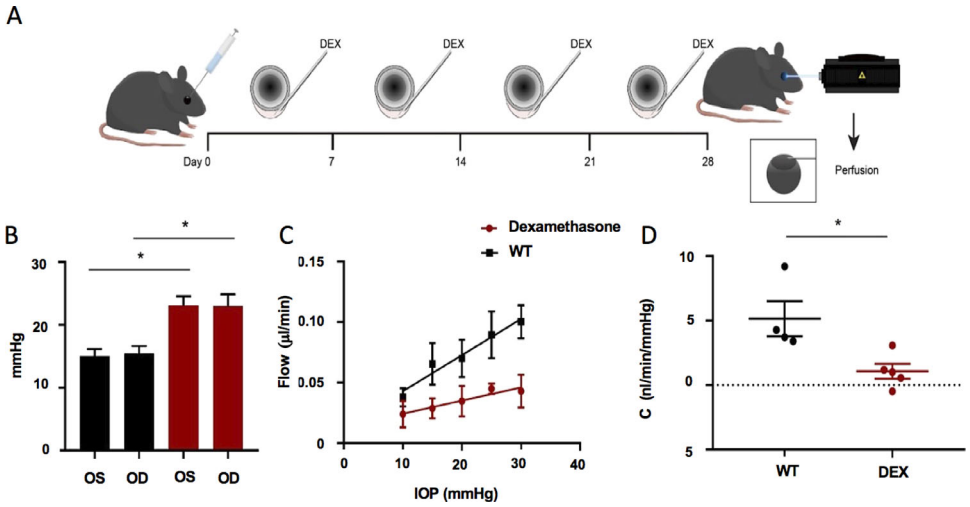

Figure 3. Dexamethasone (DEX) increases IOP by decreasing outflow facility. (A) DEX was administered by weekly subconjunctival injections using a 33G needle with a Hamilton syringe. (B) Tonometer readings showing the difference in IOP between wild-type (WT) and dexamethasone-treated mice (C) Perfusion plots of mouse eyes injected with dexamethasone and WT untreated controls. (D) DEX-treated eyes demonstrate a significantly lower outflow facility than those without exposure. ($n = 5$ mice per group, unpaired Student t-test).

Optogenetic CRY2-5-Ptase$_{OCRL}$ Stimulation Reverses Dexamethasone's Effect on Outflow Facility

To determine whether CRY2-5-ptase$_{OCRL}$ recruitment to the plasma membrane or primary cilia could modulate outflow facility in pathological conditions, we tested plasma membrane and ciliary optogenetic recruitment in the dexamethasone model. Mice were injected with viral vectors containing the relevant optogenetic constructs: AAV2-s-CRY2-5-ptase$_{OCRL}$ and AAV2-s-CIBN-EGFP-CAAX or AVV2-s-CIBN-EGFP-SSTR3 and incubated for 4 weeks. Simultaneously, to generate high IOP, dexamethasone was injected subconjunctivally into both eyes once weekly until the termination of the 4-week viral transduction period. At this time, one eye was optogenetically activated using a blue 450-nm 10-mW laser, and the other eye served as a control. Importantly, both the plasma membrane and ciliary targeting constructs significantly decreased IOP an average of 5 mm Hg in the optogenetically activated eyes (Figs. 4A, D). Perfusion data supported the results of the tonometer readings, as the light activated membrane targeting construct significantly increased outflow facility compared with no light exposure (1.2 ± 0.3 nL/min/mm Hg and 3.7 ± 1.0 nL/min/mm Hg, respectively; $P = 0.0158$; $n = 8$ mice) (Figs. 4B, C) and the light-activated ciliary targeting viral constructs also had significantly increased outflow facility compared with no light exposure (1.6 ± 0.6 nL/min/mm Hg and 7.0 ± 1.5 nL/min/mm Hg, respectively; $P = 0.0165$; n of 5 mice) (Figs. 4E, F).

Optogenetic OCRL Regulation Modulates Actin After Dexamethasone Stimulation In Vitro

Steroid exposure produces IOP elevation[57] owing to extracellular matrix accumulation in the conventional outflow pathway and TM stiffening. Cytoskeletal morphology is an indication of cell stiffness, and dexamethasone exposure induces CLANs formation in TM cells.[58] Using fluorescently tagged phalloidin, we also observed that acute treatment of HTM cells with dexamethasone (10 µM) significantly increased CLANs formation (Fig. 5A).

Because tight regulation of PI(4,5)P2 plays a significant role in modulating actin reorganization,[59,60] we analyzed whether optogenetic CRY2-5-ptase$_{OCRL}$ recruitment to the plasma membrane could rescue CLANs formation. To investigate this issue, HTM cells were transiently transfected with CRY2-5-ptase$_{OCRL}$ and CIBN-EGFP-CAAX after dexamethasone treatment. Cells were stimulated with light as described above, given 10 minutes to allow for cytoskeleton reorganization, then fixed with 4% PFA and stained with phalloidin. We observed that CRY2-5-ptase$_{OCRL}$ recruitment to the plasma membrane following blue light activation reduced the disorganized actin array and CLANs (13.0% ± 1.2% CLANs positive cells)

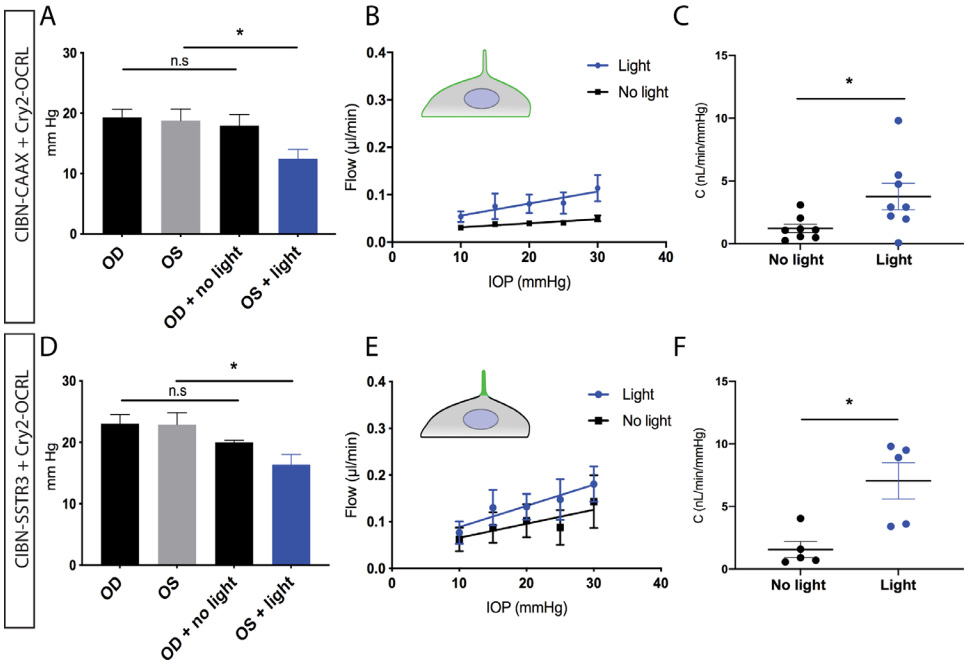

Figure 4. Dexamethasone mouse model with optogenetic reversal of IOP and outflow resistance. (A) Tonometer reading of steroid-treated mouse eyes expressing AAV2-s-CIBN-CAAX and mCh-CRY2-5-ptase$_{OCRL}$ showed a decreased IOP if they were stimulated with blue light compared with those without light exposure. (B) Perfusion plots without and with blue light exposure and (C) the calculated outflow facility showed that blue light exposure increased outflow facility for the membrane construct. Similarly, (D) tonometer readings of steroid treated mouse eyes expressing AAV2-s-CIBN-SSTR3 and mCh-CRY2-5-ptase$_{OCRL}$ with blue light exposure had a decreased IOP. (E) Perfusion plots with and without blue light exposure and (F) the calculated outflow facility showed that blue light exposure increased outflow facility for the ciliary construct. ($n = 8$ mice and 5 mice for CAAX and SSTR3 constructs respectively, paired Student *t*-test). OD, right eye; OS, left eye.

compared with transfected nonilluminated HTM cells (36.0% ± 2.6% CLANs-positive cells) (Fig. 5B, C; $P = 0.0013$; n of 3 independent experiments, counting 40 cells per group). These results support the idea that OCRL subcellular localization can modulate cytoskeletal abnormalities caused by dexamethasone exposure.

Discussion

Glaucoma is an optic neuropathy that can lead to irreversible vision loss if its primary risk factor, IOP, is not controlled. There has been increased awareness in recent years that medications, such as corticosteroids, used to treat other diseases can cause severe side effects, including the development of elevated IOP, that can lead to neuropathy categorized as glaucoma. The mechanism(s) in the conventional outflow pathway that underlie elevated IOP after steroid exposure is unclear. However, studies suggest that it might at least in part occur because corticosteroid medications can cause changes at the cellular level, including the formation of CLANs,[61–65] an increase in nucleus and cell size,[66] altered expression of extracellular matrix proteins,[67–76] inhibition of proliferation, migration,[65] and the phagocytic activity[77–80] required to clear debris from the filter-like tissue.

Previous studies in animal models have shown that treatment with steroid medications can elevate the IOP. Our present study demonstrates that treatment of wild-type mice with dexamethasone for 4 weeks is well-tolerated and sufficient to create a steroid-induced ocular hypertension model. These mice exhibited a significant decrease in outflow facility as measured by our perfusion system, resulting in increased an IOP by tonometry, consistent with the accepted characteristics of steroid-induced ocular hypertension.

Optogenetics provides a novel approach to resolving the function of proteins in disease pathogenesis. The 5-ptase domain of OCRL was cloned to light-sensitive CRY2 and expressed with its ligand (CIBN).[54] This system targets the enzyme domain to the plasma membrane, which dephosphorylates its PI(4,5)P2 and essentially depletes it of the lipid. We recently modified this system to target the 5-ptase specifically to the primary cilia, which depletes PI(4,5)P2 only in the ciliary shaft.[46] This recruitment is specifically targeted to subcellular compartments without affecting whole

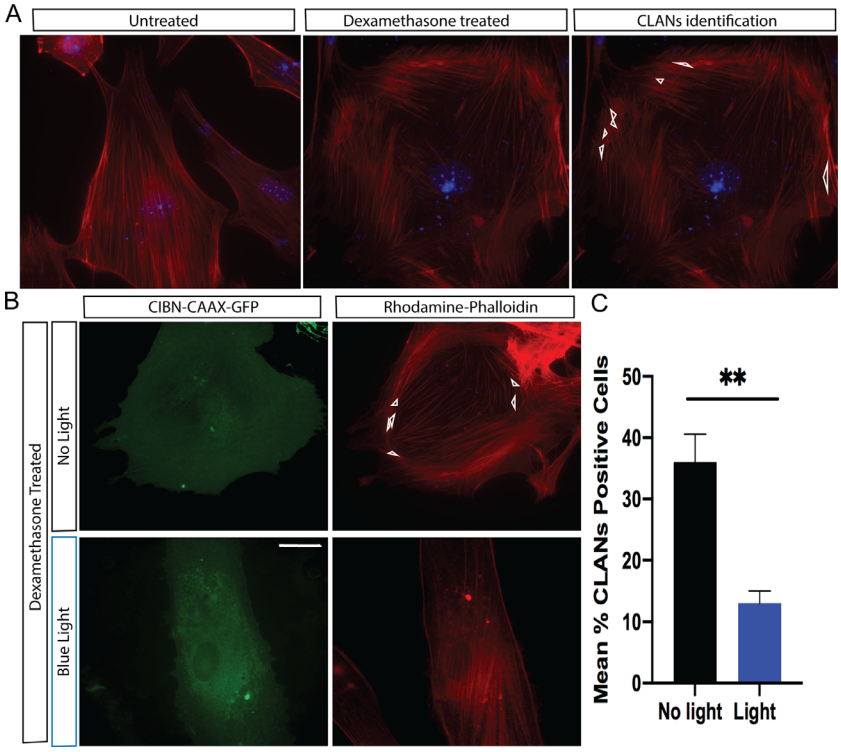

Figure 5. Optogenetic modulation of actin morphology after dexamethasone (DEX) stimulation in vitro. (A) Rhodamine-phalloidin shows the effect of DEX treatment (10 µM for 4 hours) on actin cytoskeleton organization compared with an untreated control. CLANs were identified as three bright actin filament spokes forming vertices as indicated by the white triangles. (B) HTM cells expressing CRY2-5-ptase$_{OCRL}$ and CIBN-EGFP-CAAX were treated with dexamethasone, exposed to blue light, fixed, and treated with rhodamine-phalloidin. (C) Samples optogenetically activated by blue light had a reduced number of CLANs positive cells compared with samples without blue light exposure. Scale bar = 20µm. ($n = 3$, unpaired Student's *t*-test).

cellular pathways. The system can provide novel insight into signaling mechanisms and their role in disease pathogenesis.

Because phosphoinositides are known to play critical roles in a wide range of biological processes, including membrane trafficking from the plasma membrane and regulating actin cytoskeletal organization,[59,60,81] we used the steroid-induced ocular hypertension model to assess the efficiency with which optogenetic regulation of phosphoinositide signaling counteracts the negative effect of dexamethasone. We observed that treatments to direct OCRL subcellular localization to the plasma membrane reversed the negative effects of prolonged dexamethasone exposure and decreased the IOP to nearly normal levels, suggesting that PI(4,5)P2 pools play a critical role in this mechanism of regulating IOP. Interestingly, targeting the enzymatic activity of OCRL to primary cilia produced a similar positive effect. Primary cilia are of well-known importance in sensing flow and regulating cell homeostasis[37]; our results suggest that intraciliary regulation is critical to modulating phosphoinositide function. Therefore, the regulation of phosphoinositides at both the plasma membrane and within primary cilia may participate in a converging downstream pathway, which affects cell behavior, cytoskeletal organization, homeostasis, and ultimately IOP.

$PI(4,5)P_2$ acts as a key factor in remodeling the actin cytoskeleton by regulating the activity of a number of actin-binding proteins that control the assembly of actin microfilaments.[82,83] The present report shows that dexamethasone causes severe morphological alterations in HTM cells. The cellular changes that we observed in the dexamethasone steroid-induced ocular hypertension model included a marked increase in CLANS. Dexamethasone-treated cells have been previously shown to have defects in actin,[62,65] and other studies have linked the formation of CLANs in TM cells to steroid treatment.[64,66] In addition, Filla et al[84] showed that PI(4,5)P2 colocalized at CLANs in TM cells treated with dexamethasone. The formation of CLANs is thought to significantly decrease cell plasticity,[85] and mathematical models predicting that the stiffness of actin filaments in CLANs is increased by two

orders of magnitude support this notion.[86] However, the exact mechanism and pathways regulating CLANs formation have yet to be determined.

Optogenetic recruitment of the OCRL 5-ptase, which aimed to regulate $PI(4,5)P_2$ pools at the plasma membrane or within cilia, produced actin depolymerization in dexamethasone-treated HTM cells. This result suggests that phosphoinositide regulation overcame the influence of dexamethasone to induce the cytoskeletal alterations responsible for the decrease in aqueous outflow and increase in IOP; therefore, actin represents the framework upon which IOP seems to be mediated. Other studies support this notion, particularly those focused on actin depolymerizing agents or Rho kinase inhibitors. Rho kinase inhibitors, which are among the few drugs currently under investigation for use in glaucoma, have been shown to control IOP by modulating cytoskeletal organization and decreasing the number of stress fibers and focal adhesions, which provide the cell flexibility necessary to regulate IOP.[87]

In conclusion, our study supports the hypothesis that cytoskeletal alterations and formation of CLANs act as the driving force behind the effects on outflow facility and IOP observed in the steroid-induced ocular hypertension model in vivo. Steroid medications may impair diverse actin-regulatory proteins, resulting in a TM cell and tissue environment which is stiffer and less able to dynamically regulate outflow. Subcompartmental targeting of OCRL enabled us to improve cell plasticity and thus outflow facility in the steroid-induced ocular hypertension model. This improvement coincided with a significant decrease in the number of CLANs observed in cultured HTM cells. Our study therefore provides a novel framework for a therapeutic approach based on lipid signaling and demonstrates the urgent need for future studies to determine the exact pathways involved in OCRL-dependent CLANs formation.

Acknowledgments

The authors thank Li Liang for his help with animal work.

Supported by NIH/NEI R01-EY032159 (Y.S.), R01-EY025295 (Y.S.), VA merit CX001298 (Y.S.), Children's Health Research Institute Award (Y.S.). R01-EY-023295 (Y.H.), R01-EY024932 (Y.H.), EY028106 (Y.H.), EY031063 (Y.H.), and grants from Glaucoma Research Foundation (CFC3) (Y.H.), BrightFocus Foundation (Y.H.), and Chan Zuckerberg Initiative Neurodegeneration Collaborative Pairs Pilot Projects (Y.H.). Research for Prevention of Blindness Unrestricted grant (Stanford Ophthalmology) P30 Vision Center grant to Stanford Ophthalmology department. Y.S. is a Laurie Kraus Lacob Faculty Scholar in Pediatric Translational Medicine. This work was also supported by NIH/NEI T32 training grant T32-EY027816 and F32-EY032775-01 Kirschstein-NRSA postdoctoral fellowship (T.K.).

Disclosure: **T.J. Kowal**, (N); **P.P. Prosseda**, (N); **K. Ning**, (N); **B. Wang**, (N); **J. Alvarado,** (N); **B.E. Sendayen,** (N); **S. Jabbehdari**, (N); **W.D. Stamer**, (N); **Y. Hu**, (N); **Y. Sun**, (N)

* TJK and PPP contributed equally.

References

1. Fini ME, Schwartz SG, Gao X, et al. Steroid-induced ocular hypertension/glaucoma: focus on pharmacogenomics and implications for precision medicine. *Prog Retin Eye Res*. 2017;56:58–83.
2. Ciulla TA, Walker JD, Fong DS, Criswell MH. Corticosteroids in posterior segment disease: an update on new delivery systems and new indications. *Curr Opin Ophthalmol*. 2004;15(3):211–220.
3. Al-Khersan H, Hariprasad SM, Chhablani J, Dex Implant Study Group. Early response to intravitreal dexamethasone implant therapy in diabetic macular edema may predict visual outcome. *Am J Ophthalmol*. 2017;184:121–128.
4. Miller K, Fortun JA. Diabetic macular edema: current understanding, pharmacologic treatment options, and developing therapies. *Asia Pac J Ophthalmol (Phila)*. 2018;7(1):28–35.
5. Schwartz SG, Scott IU, Stewart MW, Flynn HW. Update on corticosteroids for diabetic macular edema. *Clin Ophthalmol*. 2016;10:1723–1730.
6. Haller JA, Bandello F, Belfort R, et al. Dexamethasone intravitreal implant in patients with macular edema related to branch or central retinal vein occlusion twelve-month study results. *Ophthalmology*. 2011;118(12):2453–2460.
7. Dibas A, Yorio T. Glucocorticoid therapy and ocular hypertension. *Eur J Pharmacol*. 2016;787:57–71.
8. Miller D, Peczon JD, Whitworth CG. Corticosteroids and functions in the anterior segment of the eye. *Am J Ophthalmol*. 1965;59:31–34.
9. Kersey JP, Broadway DC. Corticosteroid-induced glaucoma: a review of the literature. *Eye (Lond)*. 2006;20(4):407–416.
10. Becker B, Podos SM, Asseff CF, Cooper DG. Plasma cortisol suppression in glaucoma. *Am J Ophthalmol*. 1973;75(1):73–76.

11. Clark AF. Basic sciences in clinical glaucoma: steroids, ocular hypertension, and glaucoma. *J Glaucoma*. 1995;4(5):354–369.
12. Goldmann H. Cortisone glaucoma. *Arch Ophthalmol*. 1962;68:621–626.
13. Francois J. [Cortisone and eye strain]. *Ann Ocul (Paris)*. 1954;187(9):805–816.
14. Bernstein HN, Schwartz B. Effects of long-term systemic steroids on ocular pressure and tonographic values. *Arch Ophthalmol*. 1962;68:742–753.
15. Schwartz B, Levene RZ. Plasma cortisol differences between normal and glaucomatous patients: before and after dexamethasone suppresion. *Arch Ophthalmol*. 1972;87(4):369–377.
16. Meyer LM, Schönfeld C-L. Secondary glaucoma after intravitreal dexamethasone 0.7 mg implant in patients with retinal vein occlusion: a one-year follow-up. *J Ocul Pharmacol Ther*. 2013;29(6):560–565.
17. Spaeth GL. Traumatic hyphema, angle recession, dexamethasone hypertension, and glaucoma. *Arch Ophthalmol*. 1967;78(6):714–721.
18. Lewis JM, Priddy T, Judd J, et al. Intraocular pressure response to topical dexamethasone as a predictor for the development of primary open-angle glaucoma. *Am J Ophthalmol*. 1988;106(5):607–612.
19. Weinreb RN, Polansky JR, Kramer SG, Baxter JD. Acute effects of dexamethasone on intraocular pressure in glaucoma. *Invest Ophthalmol Vis Sci*. 1985;26(2):170–175.
20. Armaly MF. Inheritance of dexamethasone hypertension and glaucoma. *Arch Ophthalmol*. 1967;77(6):747–751.
21. Becker B, Mills DW. Corticosteroids and intraocular pressure. *Arch Ophthalmol*. 1963;70:500–507.
22. Gerometta R, Podos SM, Danias J, Candia OA. Steroid-induced ocular hypertension in normal sheep. *Invest Ophthalmol Vis Sci*. 2009;50(2):669–673.
23. Gerometta R, Podos SM, Candia OA, et al. Steroid-induced ocular hypertension in normal cattle. *Arch Ophthalmol*. 2004;122(10):1492–1497.
24. Whitlock NA, McKnight B, Corcoran KN, Rodriguez LA, Rice DS. Increased intraocular pressure in mice treated with dexamethasone. *Invest Ophthalmol Vis Sci*. 2010;51(12):6496–6503.
25. SooHoo JR, Seibold LK, Laing AE, Kahook MY. Bleb morphology and histology in a rabbit model of glaucoma filtration surgery using Ozurdex or mitomycin-C. *Mol Vis*. 2012;18:714–719.
26. Patel GC, Phan TN, Maddineni P, et al. Dexamethasone-induced ocular hypertension in mice: effects of myocilin and route of administration. *Am J Pathol*. 2017;187(4):713–723.
27. Sawaguchi K, Nakamura Y, Nakamura Y, Sakai H, Sawaguchi S. Myocilin gene expression in the trabecular meshwork of rats in a steroid-induced ocular hypertension model. *Ophthalmic Res*. 2005;37(5):235–242.
28. Gelatt KN, Mackay EO. The ocular hypertensive effects of topical 0.1% dexamethasone in beagles with inherited glaucoma. *J Ocul Pharmacol Ther*. 1998;14(1):57–66.
29. Zhan GL, Miranda OC, Bito LZ. Steroid glaucoma: corticosteroid-induced ocular hypertension in cats. *Exp Eye Res*. 1992;54(2):211–218.
30. Li G, Lee C, Agrahari V, et al. In vivo measurement of trabecular meshwork stiffness in a corticosteroid-induced ocular hypertensive mouse model. *Proc Natl Acad Sci USA*. 2019;116(5):1714–1722.
31. Wang K, Johnstone MA, Xin C, et al. Estimating human trabecular meshwork stiffness by numerical modeling and advanced OCT imaging. *Invest Ophthalmol Vis Sci*. 2017;58(11):4809–4817.
32. Last JA, Pan T, Ding Y, et al. Elastic modulus determination of normal and glaucomatous human trabecular meshwork. *Invest Ophthalmol Vis Sci*. 2011;52(5):2147–2152.
33. Raghunathan VK, Morgan JT, Park SA, et al. Dexamethasone stiffens trabecular meshwork, trabecular meshwork cells, and matrix. *Invest Ophthalmol Vis Sci*. 2015;56(8):4447–4459.
34. Wang K, Li G, Read AT, et al. The relationship between outflow resistance and trabecular meshwork stiffness in mice. *Sci Rep*. 2018;8(1):5848.
35. Patel GC, Millar JC, Clark AF. Glucocorticoid receptor transactivation is required for glucocorticoid-induced ocular hypertension and glaucoma. *Invest Ophthalmol Vis Sci*. 2019;60(6):1967–1978.
36. Zode GS, Sharma AB, Lin X, et al. Ocular-specific ER stress reduction rescues glaucoma in murine glucocorticoid-induced glaucoma. *J Clin Invest*. 2014;124(5):1956–1965.
37. Luo N, Conwell MD, Chen X, et al. Primary cilia signaling mediates intraocular pressure sensation. *Proc Natl Acad Sci USA*. 2014;111(35):12871–12876.
38. Jalalvand E, Robertson B, Wallén P, Grillner S. Ciliated neurons lining the central canal sense both fluid movement and pH through ASIC3. *Nat Commun*. 2016;7:10002.
39. Lowe CU, Terrey M, MacLACHLAN EA. Organic-aciduria, decreased renal ammonia production, hydrophthalmos, and mental retardation;

a clinical entity. *AMA Am J Dis Child*. 1952;83(2):164–184.
40. Nussbaum RL, Orrison BM, Jänne PA, Charnas L, Chinault AC. Physical mapping and genomic structure of the Lowe syndrome gene OCRL1. *Hum Genet*. 1997;99(2):145–150.
41. Zhang X, Jefferson AB, Auethavekiat V, Majerus PW. The protein deficient in Lowe syndrome is a phosphatidylinositol-4,5-bisphosphate 5-phosphatase. *Proc Natl Acad Sci USA*. 1995;92(11): 4853–4856.
42. Attree O, Olivos IM, Okabe I, et al. The Lowe's oculocerebrorenal syndrome gene encodes a protein highly homologous to inositol polyphosphate-5-phosphatase. *Nature*. 1992;358(6383):239–242.
43. Schmid AC, Wise HM, Mitchell CA, Nussbaum R, Woscholski R. Type II phosphoinositide 5-phosphatases have unique sensitivities towards fatty acid composition and head group phosphorylation. *FEBS Lett*. 2004;576(1-2):9–13.
44. Morgan JT, Wood JA, Walker NJ, et al. Human trabecular meshwork cells exhibit several characteristics of, but are distinct from, adipose-derived mesenchymal stem cells. *J Ocul Pharmacol Ther*. 2014;30(2-3):254–266.
45. Keller KE, Bhattacharya SK, Borrás T, et al. Consensus recommendations for trabecular meshwork cell isolation, characterization and culture. *Exp Eye Res*. 2018;171:164–173.
46. Prosseda PP, Alvarado JA, Wang B, et al. Optogenetic stimulation of phosphoinositides reveals a critical role of primary cilia in eye pressure regulation. *Sci Adv*. 2020;6(18):eaay8699.
47. Filla MS, Schwinn MK, Sheibani N, Kaufman PL, Peters DM. Regulation of Cross-linked Actin Network (CLAN) formation in Human Trabecular Meshwork (HTM) cells by convergence of distinct β1 and β3 integrin pathways. *Invest Ophthalmol Vis Sci*. 2009;50(12):5723–5731.
48. Ko MK, Yelenskiy A, Gonzalez JM, Jr, Tan JCH. Feedback-controlled constant-pressure anterior chamber perfusion in live mice. *Mol Vis*.2014;20:163–170.
49. Wang Q, Wu Z, Zhang J, et al. A robust system for production of superabundant VP1 recombinant AAV vectors. *Mol Ther Methods Clin Dev*. 2017;7:146–156.
50. Boussommier-Calleja A, Bertrand J, Woodward DF, Ethier CR, Stamer WD, Overby DR. Pharmacologic manipulation of conventional outflow facility in ex vivo mouse eyes. *Invest Ophthalmol Vis Sci*. 2012;53(9):5838–5845.
51. Ko MK, Yelenskiy A, Gonzalez JM, Tan JCH. Feedback-controlled constant-pressure anterior chamber perfusion in live mice. *Mol Vis*. 2014;20:163–170.
52. Bogner B, Boye SL, Min SH, et al. Capsid mutated adeno-associated virus delivered to the anterior chamber results in efficient transduction of trabecular meshwork in mouse and rat. *PLoS ONE*. 2015;10(6):e0128759.
53. Lock M, Alvira M, Vandenberghe LH, et al. Rapid, simple, and versatile manufacturing of recombinant adeno-associated viral vectors at scale. *Hum Gene Ther*. 2010;21(10):1259—1271.
54. Idevall-Hagren O, Decamilli P. Manipulation of plasma membrane phosphoinositides using photoinduced protein-protein interactions. *Methods Mol Biol*. 2014;1148:109–128.
55. Berbari NF, Johnson AD, Lewis JS, Askwith CC, Mykytyn K. Identification of ciliary localization sequences within the third intracellular loop of G protein-coupled receptors. *Mol Biol Cell*. 2008;19(4):1504–1507.
56. Nachury M V., Seeley ES, Jin H. Trafficking to the ciliary membrane: how to get across the periciliary diffusion barrier? *Annu Rev Cell Dev Bio*. 2010;26:59–87.
57. Weinreb RN, Polansky JR, Kramer SG, Baxter JD. Acute effects of dexamethasone on intraocular pressure in glaucoma. *Invest Ophthalmol Vis Sci*. 1985;26(2):170–175.
58. Montecchi-Palmer M, Bermudez JY, Webber HC, Patel GC, Clark AF, Mao W. TGFβ2 induces the formation of cross-linked actin networks (CLANs) in human trabecular meshwork cells through the smad and non-smad dependent pathways. *Invest Ophthalmol Vis Sci*. 2017;58(2):1288–1295.
59. Hayes MJ, Shao D-M, Grieve A, Levine T, Bailly M, Moss SE. Annexin A2 at the interface between F-actin and membranes enriched in phosphatidylinositol 4,5,-bisphosphate. *Biochim Biophys Acta*. 2009;1793(6):1086–1095.
60. Suchy SF, Nussbaum RL. The deficiency of PIP2 5-phosphatase in Lowe syndrome affects actin polymerization. *Am J Hum Genet*. 2002;71(6):1420–1427.
61. Bermudez JY, Montecchi-Palmer M, Mao W, Clark AF. Cross-linked actin networks (CLANs) in glaucoma. *Exp Eye Res*. 2017;159:16–22.
62. Clark AF, Brotchie D, Read AT, et al. Dexamethasone alters F-actin architecture and promotes cross-linked actin network formation in human trabecular meshwork tissue. *Cell Motil Cytoskeleton*. 2005;60(2):83–95.
63. Hoare M-J, Grierson I, Brotchie D, Pollock N, Cracknell K, Clark AF. Cross-linked actin

networks (CLANs) in the trabecular meshwork of the normal and glaucomatous human eye in situ. *Invest Ophthalmol Vis Sci*. 2009;50(3):1255–1263.
64. O'Reilly S, Pollock N, Currie L, Paraoan L, Clark AF, Grierson I. Inducers of cross-linked actin networks in trabecular meshwork cells. *Invest Ophthalmol Vis Sci*. 2011;52(10):7316–7324.
65. Clark AF, Wilson K, McCartney MD, Miggans ST, Kunkle M, Howe W. Glucocorticoid-induced formation of cross-linked actin networks in cultured human trabecular meshwork cells. *Invest Ophthalmol Vis Sci*. 1994;35(1):281–294.
66. Wordinger RJ, Clark AF. Effects of glucocorticoids on the trabecular meshwork: towards a better understanding of glaucoma. *Prog Retin Eye Res*. 1999;18(5):629–667.
67. Roll P, Benedikt O. [Electronmicroscopic studies of the trabecular meshwork in corticosteroid glaucoma]. *Klin Monbl Augenheilkd*. 1979;174(3):421–428.
68. Rohen JW, Linnér E, Witmer R. Electron microscopic studies on the trabecular meshwork in two cases of corticosteroid-glaucoma. *Exp Eye Res*. 1973;17(1):19–31.
69. Johnson DH, Bradley JM, Acott TS. The effect of dexamethasone on glycosaminoglycans of human trabecular meshwork in perfusion organ culture. *Invest Ophthalmol Vis Sci*. 1990;31(12):2568–2571.
70. Steely HT, Browder SL, Julian MB, Miggans ST, Wilson KL, Clark AF. The effects of dexamethasone on fibronectin expression in cultured human trabecular meshwork cells. *Invest Ophthalmol Vis Sci*. 1992;33(7):2242–2250.
71. Dickerson JE, Steely HT, English-Wright SL, Clark AF. The effect of dexamethasone on integrin and laminin expression in cultured human trabecular meshwork cells. *Exp Eye Res*. 1998;66(6):731–738.
72. Zhou L, Li Y, Yue BY. Glucocorticoid effects on extracellular matrix proteins and integrins in bovine trabecular meshwork cells in relation to glaucoma. *Int J Mol Med*. 1998;1(2):339–346.
73. Yun AJ, Murphy CG, Polansky JR, Newsome DA, Alvarado JA. Proteins secreted by human trabecular cells. Glucocorticoid and other effects. *Invest Ophthalmol Vis Sci*. 1989;30(9):2012–2022.
74. Toriyama K. An Electron microscopic study of the trabecular meshwork in corticosteroid-glaucoma. *Folia Ophthalmol Jopn*. 1979;30:1583–1589.
75. Luten-Drescoll E, Rohen JW. Morphology of aqueous outflow pathways in normal and glaucotomous eyes. In: *The Glaucomas*. Vol. 1. Ritch R, Sheilds MB, Krupin T, authors. Highlands, NJ: The C.V. Mosby Cp.; 1989:41–74.
76. Polansky JR, Fauss DJ, Chen P, et al. Cellular pharmacology and molecular biology of the trabecular meshwork inducible glucocorticoid response gene product. *Ophthalmologica*. 1997;211(3):126–139.
77. Zhang X, Ognibene CM, Clark AF, Yorio T. Dexamethasone inhibition of trabecular meshwork cell phagocytosis and its modulation by glucocorticoid receptor beta. *Exp Eye Res*. 2007;84(2):275–284.
78. Shirato S, Bloom E, Polansky J, Alvarado J, Stilwell L. Phagocytic properties of confluent cultured human trabecular meshwork cells. *Invest Ophthalmol Vis Sci*. 1988;29:S125.
79. Polansky JR, Kurtz RM, Fauss DJ, Kim RY, Bloom E. In vitro correlates of glucocorticoid effects on intraocular pressure. In: Krieglstein GK, ed. *Glaucoma Update IV*. Heidelberg: Springer; 1991:20–29.
80. Matsumoto Y, Johnson DH. Dexamethasone decreases phagocytosis by human trabecular meshwork cells in situ. *Invest Ophthalmol Vis Sci*. 1997;38:1902–1907.
81. Mehta ZB, Pietka G, Lowe M. The cellular and physiological functions of the Lowe syndrome protein OCRL1. *Traffic*. 2014;15(5):471–487.
82. Logan MR, Mandato CA. Regulation of the actin cytoskeleton by PIP2 in cytokinesis. *Biol Cell*. 2006;98(6):377–388.
83. Yin HL, Janmey PA. Phosphoinositide regulation of the actin cytoskeleton. *Annu Rev Physiol*. 2003;65:761–789.
84. Filla MS, Schwinn MK, Nosie A K, Clark RW, Peters DM. Dexamethasone-associated cross-linked actin network formation in human trabecular meshwork cells involves β3 integrin signaling. *Invest Ophthalmol Vis Sci*. 2011;52(6):2952–2959.
85. Fifková E, Delay RJ. Cytoplasmic actin in neuronal processes as a possible mediator of synaptic plasticity. *J Cell Biol*. 1982;95(1):345–350.
86. Gardel ML, Shin JH, MacKintosh FC, Mahadevan L, Matsudaira P, Weitz DA. Elastic behavior of cross-linked and bundled actin networks. *Science*. 2004;304(5675):1301–1305.
87. Van de Velde S, Van Bergen T, Sijnave D, et al. AMA0076, a novel, locally acting rho kinase inhibitor, potently lowers intraocular pressure in New Zealand white rabbits with minimal hyperemia. *Invest Ophthalmol Vis Sci*. 2014;55(2):1006–1016.